Polyhedron 187 (2020) 114631

Contents lists available at ScienceDirect

Polyhedron

journal homepage: www.elsevier.com/locate/poly

A hemilabile diphosphine pyridine pincer ligand: σ- and π-binding in molybdenum coordination complexes

Ruomeng Wan, Joshua A. Buss, Kyle T. Horak, Theodor Agapie *

Division of Chemistry and Chemical Engineering, California Institute of Technology, 1200 East California Boulevard, MC 127-72, Pasadena, CA 91125, United States

ARTICLE INFO

Article history:
Received 5 February 2020
Accepted 29 May 2020
Available online 4 June 2020

Dedicated to John Bercaw on the occasion of his 75th birthday. Thank you, John, for your inspiring science, mentorship, and friendship!

Keywords:
Hemilabile ligands
Pincer complexes
Molybdenum
Transition metal nitride

ABSTRACT

A series of molybdenum compounds supported by a hemilabile pyridine diphosphine pincer ligand have been synthesized. The ligand demonstrates variable binding modes, adapting to the electronic and geometric requirements of the metal center. In Mo^0 and Mo^{II} polycarbonyl complexes, coordination through the σ-donating pyridine nitrogen lone pair is observed. Upon oxidative group transfer with anionic azide, a Mo^{IV} nitride compound is formed, accompanied by a change in the ancillary ligand binding mode to the pyridine π-system. The σ-coordination was restored by subsequent functionalization of the nitride moiety with either silyl electrophiles or protons. Protonation results in redox disproportionation with concomitant nitride functionalization. Characterization by single crystal X-ray diffraction, nuclear magnetic resonance, and infrared spectroscopy is discussed.

1. Introduction

The tridentate pincer ligand has been established as a "privileged" ligand scaffold [1] due to its versatility in coordination chemistry and homogeneous catalysis applications: [2] from studies in the 1970s of PCP- and NCN-pincer metal complexes [3,4] relevant to C—C bond formation [5], to the more recent applications of PNP-pincer metal complexes in N_2 fixation-related chemistry [6,7]. Although the pincer scaffold's rigid binding plays a critical role in the durability of many catalytic systems [8], the potential flexibility of this ligand platform can also be an asset to reactivity [9]. Hemilability [10], a design feature frequently observed in nature [11–13], has been shown to induce higher selectivity and activity in molecular catalysts by enabling the ligands to adapt to changes in oxidation state at the metal center and to control the accessibility of open coordination sites [14–17].

Our laboratory has reported a series of diphosphine arene pincer ligands [18] that display hemilabile coordination [19], and under strongly reducing conditions, redox non-innocence [20]. More recently, we have found that changing the identity of the central aryl linker allows for both remote tuning of the electronics at the metal center [21] and multi-electron multi-proton chemistry under mild conditions [22]. Metal complexes supported by these ligands perform a variety of stoichiometric or catalytic chemical transformations including CO_2 reduction [23], CO coupling [20(b),24,25], alkyne-nitrile cotrimerization [26], O_2 reduction [27], phosphide coupling [28], and nitride-CO coupling [29]. With demonstrated relevance of PNP ligand platforms to small molecule activation [30], in particular N_2 reduction catalysis [6,7], we are interested in exploring the chemistry of Mo complexes featuring a teraryl ligand platform incorporating a PNP-type motif [6]. The challenging six electron six proton process [31] involved in N_2 reduction to ammonia may require a range of oxidation states at the metal center [32,33], a demanding reactivity sequence that could potentially be better supported by a hemilabile ligand [34]. We envisioned that utilizing a 2,6-substituted pyridine in the central linking position of a teraryl diphosphine might facilitate two modes of pyridine binding (Scheme 1) depending on the electronic requirements of and coordination geometries at the metal ion: A) nitrogen σ-binding (**σ-Py**), as is observed in archetypal PNP ligands, [6(a)] and B) pyridine π-system coordination, imposed by the strained phenylene bridges (**π-Py**) [19(d)]. Herein, we discuss the synthesis of Mo complexes supported by a flexible P-pyridine-P pincer scaffold that demonstrates σ- and π-coordination.

2. Experimental

2.1. General considerations

Unless otherwise specified, all operations were carried out in an MBraun glovebox under a nitrogen atmosphere or using standard

* Corresponding author.
E-mail address: agapie@caltech.edu (T. Agapie).

https://doi.org/10.1016/j.poly.2020.114631
0277-5387/

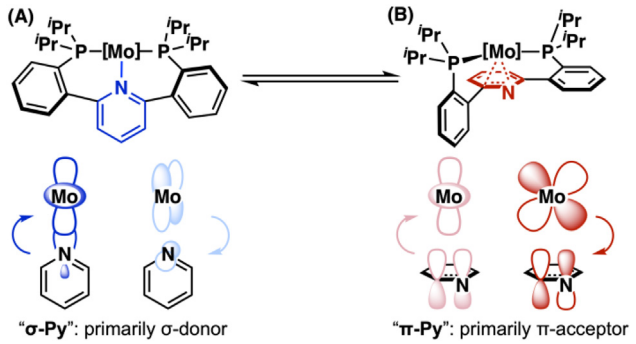

Scheme 1. The σ- and π-binding modes of the hemilabile diphosphine pyridine ligand.

Schlenk and vacuum line techniques. Solvents for air- and moisture- sensitive reactions were dried over sodium benzophenone ketyl, calcium hydride, or by the method of Grubbs [35]. Deuterated solvents were purchased from Cambridge Isotope Laboratories and vacuum transferred from sodium benzophenone ketyl or calcium hydride. Solvents, once dried and degassed, were stored under inert atmosphere over activated 4 Å molecular sieves. Tris (acetonitrile)tricarbonyl-molybdenum ($Mo(CO)_3(MeCN)_3$) [36] and $HBAr^F_4{\cdot}Et_2O$ ($[BAr^F_4]$ = $[3,5\text{-}(CF_3)_2\text{-}C_6H_3]_4B]^-$) [37], were prepared and purified according to literature procedures. Unless indicated otherwise, all other chemicals were utilized as received. $Mo(CO)_6$ and $Pd(PPh_3)_4$ were purchased from Strem Chemicals, Inc. Triphenylsilyl chloride (sublimed prior to use), tetrabutylammonium (TBA) azide (dried under vac. at 40 °C for 8 h), 1.7 M ^{t}BuLi in pentane, *2,6*-dibromopyridine and chlorodiisopropylphosphine were purchased from Sigma-Aldrich. *2*-bromophenylboronic acid was purchased from Ark Pharm, Inc. K_2CO_3 was purchased from Chem-Impex Int'l. Inc. Trimethylsilyl chloride (dried over CaH_2 and distilled prior to use) and silver trifluoromethanesulfonate (triflate, OTf) were purchased from Alfa Aesar. ^{1}H, ^{13}C{^{1}H}, and ^{31}P{^{1}H} NMR spectra were recorded on Varian 400 MHz or Varian INOVA-500 MHz spectrometers with shifts reported in parts per million (ppm). ^{1}H and ^{13}C{^{1}H} NMR spectra are referenced to residual proteo solvent and the deuterated solvent resonances, respectively [38]. ^{31}P{^{1}H} chemical shifts are referenced to an external 85% H_3PO_4 (0 ppm) standard. Multiplicities are abbreviated as follows: s = singlet, d = doublet, t = triplet, q = quartet, sep = septet, dd = doublet of doublets, m = multiplet, br = broad, v br = very broad (multiplicity assignments are omitted for "br" and "v br" assignments due to poor resolution). Powder and thin film ATR-IR measurements were obtained by placing a powder or drop of solution of the complex on the surface of a Bruker APLHA ATR-IR spectrometer probe and allowing the solvent to evaporate (Platinum Sampling Module, diamond, OPUS software package) at 2 cm^{-1} resolution. Photolyses were conducted in quartz vessels using an Oriel Instruments arc lamp housing and a Newport Corporation 200 W Hg/Xe arc lamp set to a current of 8 A. During irradiation, samples were cooled with a dry ice/acetone bath. Elemental analysis was performed at the Caltech XRCF using a PerkinElmer 2400 Series II CHN Elemental Analyzer.

2.2. Synthesis of the complexes

2.2.1. Preparation of 2,6-bis(2-bromophenyl)pyridine

Suzuki coupling conditions were adapted from a previously published procedure [39]. 2,6-dibromopyridine (11.23 g, 47.42 mmol), 2-bromo-phenylboronic acid (20.00 g, 99.59 mmol), K_2CO_3 (39.33 g, 284.53 mmol), 700 mL toluene, 200 mL ethanol, 200 mL water and a stir bar were added to a 1.5 L Schlenk flask fitted with a screw-in Teflon stopper. The mixture was degassed, and $Pd(PPh_3)_4$ (2.74 g, 2.37 mmol) was added with a counterflow of nitrogen. The reaction vessel was placed in an oil bath preheated at 75 °C. After stirring for 48 h, the reaction mixture was cooled to room temperature to provide a yellow suspension. Volatiles were removed via rotary evaporation, affording light yellow solids. Water (100 mL) was added to these solids, and the resulting mixture was extracted with CH_2Cl_2 (3 × 100 mL), dried over $MgSO_4$, filtered through Celite, and concentrated by rotary evaporation. Recrystallization from CH_2Cl_2/MeOH, followed by a MeOH wash and drying under vacuum overnight yielded white crystals of *2,6*-bis(*2*-bromophenyl)pyridine (11.28 g, 28.93 mmol, 61%). ^{1}H NMR (400 MHz, C_6D_6, 25 °C) δ: 7.58 (d, *J* = 7.6 Hz, 2H, aryl-*H*), 7.46 (d, *J* = 7.9 Hz, 2H, aryl-*H*), 7.37 (d, *J* = 7.6 Hz, 2H, central pyridine-*H*), 7.22 (t, *J* = 7.6 Hz, 1H, central pyridine-*H*), 6.97 (t, *J* = 7.5 Hz, 2H, aryl-*H*), 6.74 (t, *J* = 7.8 Hz, 2H, aryl-*H*). ^{13}C{^{1}H} NMR (126 MHz, C_6D_6, 25 °C) δ: 158.2 (s, central pyridine-*C*), 135.6 (s, aryl-*C*), 133.5 (s, aryl-*C*), 132.5 (s, aryl-*C*), 129.8 (s, aryl-*C*) 127.6 (s, aryl-*C*), 123.5 (s, central pyridine-*C*), 122.2 (s, aryl-*C*). MS (*m*/*z*): calcd, 389.9316 (M^+); found, 389.9328 (FAB-MS, M^+).

2.2.2. Preparation of 2,6-bis(2-(diisopropylphosphaneyl)- phenyl) pyridine (**1**)

2,6-bis(*2*-bromophenyl)pyridine (17.83 g, 45.82 mmol) was dissolved in tetrahydrofuran (THF) (250 mL) and loaded into a Schlenk flask charged with a magnetic stir bar and fitted with a screw-in Teflon stopper. After the reaction mixture was cooled in a dry ice-acetone bath to −78 °C, ^{t}BuLi (12.03 g in 110.5 mL pentanes, 1.7 M, 187.88 mmol) was slowly added via cannula transfer. The resulting mixture was stirred at −78 °C for 2 h, furnishing a deep red solution. Chlorodiisopropylphosphine (100.81 mmol, 16.04 mL) was then added to the reaction mixture at −78 °C via syringe. After stirring the reaction at −78 °C for 16 h, the mixture was allowed to warm to room temperature, and volatiles were removed under reduced pressure to yield orange brown solids. Degassed H_2O (200 mL) and degassed CH_2Cl_2 (200 mL) were added to these solids in a glove box, and the organic phase collected. The aqueous phase was extracted with CH_2Cl_2 two more times (2 × 200 mL). The combined organic fractions were dried over $MgSO_4$, filtered, and the volatiles were removed under reduced pressure to provide bright orange solids. These solids were washed with acetonitrile (3 × 50 mL) until the washes appeared colorless. The resultant white solids were dried under reduced pressure, affording analytically pure *2,6*-bis(*2*-(diisopropylphosphaneyl)phenyl) pyridine (**1**, 13.59 g, 29.32 mmol, 64%). ^{1}H NMR (500 MHz, C_6D_6, 25 °C) δ: 7.77–7.75 (m, 2H, aryl-*H*), 7.48 (br s, 2H, aryl-*H*), 7.47 (br s, 2H, central pyridine-*H*), 7.31 (t, *J* = 7.7 Hz, 1H, central pyridine-*H*), 7.23–7.26 (m, 2H, aryl-*H*), 7.19–7.22 (m, 2H, aryl-*H*), 1.97–2.03 (m, 4H, C*H*$(CH_3)_2$), 1.04 (dd, *J* = 13.9 Hz, 7.0 Hz, 12H, CH$(CH_3)_2$), 0.94 (dd, *J* = 12.0 Hz, 7.0 Hz, 12H, CH$(CH_3)_2$). ^{13}C{^{1}H} NMR (126 MHz, C_6D_6, 25 °C) δ: 159.6 (d, *J* = 3.9 Hz, central pyridine-*C*), 149.8 (d, *J* = 26.3 Hz, aryl-*C*), 135.8 (d, *J* = 24.9 Hz, aryl-*C*), 134.0 (s, central pyridine-*C*), 132.6 (d, *J* = 3.0 Hz, aryl-*C*), 131.2 (d, *J* = 5.2 Hz, aryl-*C*), 128.5, (s, aryl-*C*), 127.5 (s, aryl-*C*), 124.3 (d, *J* = 8.0 Hz, central pyridine-*C*), 25.0 (d, *J* = 15.7 Hz, *C*H$(CH_3)_2$), 20.4 (d, *J* = 6.7 Hz, CH$(CH_3)_2$), 20.3 (s, CH$(CH_3)_2$). ^{31}P{^{1}H} NMR (121 MHz, C_6D_6, 25 °C) δ: −2.64. Anal. Calcd. for **1** $C_{29}H_{39}NP_2$ (%): C, 75.14; H, 8.48; N, 3.02. Found: C, 75.14; H, 8.75; N, 3.03.

2.2.3. Preparation of **2**

A Schlenk tube fitted with a screw-in Teflon stopper was charged with **1** (2.51 g, 3.90 mmol), $Mo(CO)_3(MeCN)_3$ (1.18 g, 3.90 mmol), toluene (150 mL) and a stir bar. An immediate color change to orange was observed after stirring was initiated. Stirring was continued at room temperature for 48 h, providing a bright orange suspension. The volume of toluene was reduced *in vacuo*

to 20 mL to precipitate additional orange powder, **2**, which was collected on a fritted glass funnel via vacuum filtration (2.13 g, 3.32 mmol, 85%). X-ray quality crystals of **2** were grown by vapor diffusion of hexanes into a concentrated benzene solution. ^{1}H NMR (500 MHz, CD_2Cl_2, 25 °C) δ: 7.74 (t, *J* = 7.8 Hz, 1H, central pyridine-*H*), 7.46–7.50 (m, 6H, aryl-*H*), 7.28–7.30 (m, 2H, aryl-*H*), 7.21 (d, *J* = 7.8 Hz, 2H, central pyridine-*H*), 2.89–2.97 (m, 2H, C*H*$(CH_3)_2$), 1.77–1.86 (m, 2H, C*H*$(CH_3)_2$), 1.52–1.56 (m, 6H, CH(C*H*$_3)_2$), 1.35–1.40 (m, 6H, CH(C*H*$_3)_2$), 1.09–1.12 (m, 6H, CH(C*H*$_3)_2$), 0.63–0.67 (m, 6H, CH(C*H*$_3)_2$). ^{13}C{^{1}H} NMR (126 MHz, CD_2Cl_2, 25 °C) δ: 228.6 (t, *J* = 7.0 Hz, Mo-*C*O), 218.5–219.0 (m, Mo-*C*O), 162.1 (s, central pyridine-*C*), 146.9 (t, *J* = 8.7 Hz, aryl-*C*), 137.8 (s, central pyridine-*C*), 135.0–135.2 (m, aryl-*C*), 134.1 (s, aryl-*C*), 128.9 (s, aryl-*C*), 128.5 (s, aryl-*C*), 128.1 (s, aryl-*C*), 127.8 (s, central pyridine-*C*), 27.0 (s, C*H*$(CH_3)_2$), 23.8–23.9 (m, C*H*$(CH_3)_2$), 19.8 (s, CH(C*H*$_3)_2$), 19.1 (s, CH(C*H*$_3)_2$), 18.9 (s, CH(C*H*$_3)_2$), 18.7 (s, CH(C*H*$_3)_2$). ^{31}P{^{1}H} NMR (121 MHz, CD_2Cl_2, 25 °C) δ: 35.04. IR (ATR, cm^{-1}) ν_{CO}: 1910, 1815, 1796. Anal. Calcd. for **2** $C_{32}H_{39}MoO_3P_2N$ (%): C, 59.72; H, 6.11; N, 2.18. Found: C, 59.54; H, 6.12; N, 2.12.

2.2.4. Preparation of **3**

A Teflon stoppered Schenk flask was charged with **2** (510 mg, 0.79 mmol), THF (150 mL) and a stir bar. Upon initiation of stirring, a THF solution (50 mL) of AgOTf (405 mg, 1.58 mmol) was rapidly added via cannula transfer. An immediate color change from bright orange to dark green was observed. Immediately following this addition, hexanes (200 mL) was cannula transferred into the stirring reaction, furnishing green precipitate and a brown solution. The precipitate was collected via vacuum filtration on a fritted glass funnel, extracted with CH_2Cl_2 (3 × 20 mL) and filtered through Celite. The resulting green solution was dried *in vacuo* to provide **3** as a green powder (354 mg, 0.39 mmol, 49%). X-ray quality crystals of **3** were grown from vapor diffusion of hexanes into a concentrated CH_2Cl_2 solution. ^{1}H NMR (500 MHz, CD_2Cl_2, 25 °C) δ: 8.49–8.52 (m, 2H, overlapping central pyridine-*H* and aryl-*H*), 8.38 (t, *J* = 8.0 Hz, 1H, aryl-*H*), 8.13–8.14 (m, 2H, overlapping central pyridine-*H* and aryl-*H*), 8.04 (t, *J* = 7.7 Hz, 1H, central pyridine-*H*), 7.90 (d, *J* = 8.1 Hz, 1H, aryl-*H*), 7.85–7.86 (m, 2H, aryl-*H*), 7.75–7.78 (m, 1H, aryl-*H*), 7.66 (t, *J* = 8.2 Hz, 1H, aryl-H), 3.28–3.36 (m, 1H, C*H*$(CH_3)_2$), 3.22 (sep, *J* = 6.98 Hz, C*H*$(CH_3)_2$), 2.89–2.94 (m, 1H, C*H*$(CH_3)_2$), 2.01–2.09 (m, 1H, C*H*$(CH_3)_2$), 1.78 (dd, *J* = 19.5 Hz, 7.2 Hz, 3H, CH(C*H*$_3)_2$), 1.68 (dd, *J* = 16.6 Hz, 7.2 Hz, 3H, CH(C*H*$_3)_2$), 1.32–1.42 (m, 6H, CH(C*H*$_3)_2$), 1.11 (dd, *J* = 14.1 Hz, 6.8 Hz, 3H, CH(C*H*$_3)_2$), 1.03 (dd, *J* = 18.5 Hz, 7.3 Hz, 3H, CH(C*H*$_3)_2$), 0.83 (dd, *J* = 17.8 Hz, 7.3 Hz, 3H, CH(C*H*$_3)_2$), 0.45 (dd, *J* = 17.7 Hz, 6.9 Hz, 3H, CH(C*H*$_3)_2$). ^{13}C{^{1}H} NMR (126 MHz, CD_2Cl_2, 25 °C) δ: 234.8–235.6 (m, Mo-*C*O), 217.6–217.7 (m, Mo-*C*O), 161.3 (d, *J* = 3.6 Hz, aryl-*C*), 159.6 (d, *J* = 1.5 Hz, aryl-*C*), 150.6 (d, *J* = 1.7 Hz, central pyridine-*C*), 144.9 (d, *J* = 6.2 Hz, central pyridine-*C*), 143.9 (s, aryl-*C*), 143.1 (s, aryl-*C*), 142.2 (d, *J* = 9.9 Hz, aryl-*C*), 136.2 (d, *J* = 8.0 Hz, aryl-*C*), 134.2 (d, *J* = 5.3 Hz, central pyridine-*C*), 133.9 (s, central pyridine-*C*), 133.9–133.9 (m, aryl-*C*), 131.5 (m, aryl-*C*), 131.4 (d, *J* = 6.4 Hz, aryl-*C*), 129.1 (s, aryl-*C*), 127.1 (s, aryl-*C*), 123.2 (d, *J* = 36.0 Hz, Mo-aryl-*C*), 118.7 (q, *J* = 318.4 Hz, $F_3CSO_3^-$), 96.2–96.3 (m, central pyridine-*C*), 34.6 (d, *J* = 26.6 Hz, C*H*$(CH_3)_2$), 29.2 (d, *J* = 16.6 Hz, C*H*$(CH_3)_2$), 28.8 (d, *J* = 18.7 Hz, C*H*$(CH_3)_2$), 25.7 (d, *J* = 25.6 Hz, C*H*$(CH_3)_2$), 21.7 (d, *J* = 5.7 Hz, CH(C*H*$_3)_2$), 21.1 (d, *J* = 5.2 Hz, CH(C*H*$_3)_2$), 20.4 (s, CH(C*H*$_3)_2$), 20.0 (s, CH(C*H*$_3)_2$), 19.4 (s, CH(C*H*$_3)_2$), 19.3 (s, CH(C*H*$_3)_2$), 17.5 (d, *J* = 7.5 Hz, CH(C*H*$_3)_2$), 17.3 (d, *J* = 4.9 Hz, CH(C*H*$_3)_2$). ^{31}P{^{1}H} NMR (121 MHz, CD_2Cl_2, 25 °C) δ: 112.14 (d, *J* = 26.3 Hz), 52.41 (d, *J* = 26.4 Hz). ^{19}F{^{1}H} NMR (376 MHz, CD_2Cl_2, 25 °C) δ: −77.15 (s), −78.91(s). IR (ATR, cm^{-1}) ν_{CO}: 1966, 1898. Anal. Calcd. for **3** $C_{33}H_{39}F_6MoO_8P_2NS_2$ (%): C, 40.89; H, 4.30; N, 1.40. Found: C, 41.02; H, 4.29; N, 1.51.

2.2.5. Preparation of **4**

A solution of **3** (155 mg, 0.17 mmol) in acetonitrile (25 mL) was transferred to a quartz Schlenk tube charged with a stir bar. After being degassed via three freeze–pump–thaw cycles, the Schlenk tube was cooled in a dry ice/acetone slush bath and irradiated with a 200 W Hg/Xe lamp with stirring. During the irradiation, the Schlenk tube was degassed at regular 2 h intervals to remove liberated CO. With continued irradiation over 12 h, the solution gradually changed color from green to brown, and then to dark green. The irradiation/degas cycle was continued until ^{1}H NMR of the mixture showed a clean conversion into paramagnetic species (generally 12 – 16 h). The acetonitrile solution was concentrated under reduced pressure to 5 mL, and diethyl ether (40 mL) was added to the concentrated solution, furnishing dark green precipitate and a brown solution. The precipitate was collected on a fritted glass funnel via vacuum filtration, and washed with THF until the filtrate was colorless, yielding **4** as a microcrystalline solid (106 mg, 0.11 mmol, 64%). X-ray quality crystals were grown by vapor diffusion of ether into a concentrated acetonitrile solution of **4**. ^{1}H NMR (500 MHz, CD_3CN, 25 °C) δ: 71.05, 34.57, 21.41, 14.99, 13.17, 11.29, 10.16, 7.15, 5.75, 3.16, −2.77, −55.60, −152.77, −153.31. ^{13}C NMR and ^{31}P NMR were not collected as compound **4** is a paramagnetic species. Anal. Calcd. for **4** $C_{37}H_{48}F_6MoO_6P_2N_4S_2$ (%): C, 45.31; H, 4.93; N, 5.71. Found: C, 45.68; H, 5.17; N, 6.01.

2.2.6. Preparation of **5**

A Teflon stoppered Schlenk tube charged with **4** (400 mg, 0.41 mmol), acetonitrile (250 mL), and a stir bar was cooled to −78 °C. $TBAN_3$ (232 mg, 0.82 mmol) was dissolved in 100 mL THF, loaded into another Teflon stoppered Schlenk tube, and added into the frozen solution of **4** by cannula transfer. The reaction mixture was slowly warmed up to room temperature with stirring, during which time a color change from dark green to deep red was observed. After stirring at room temperature for 1 h, the reaction volume was reduced *in vacuo* to *ca.* 50 mL, and pentane (350 mL) was cannula transferred into the reaction mixture to afford a black precipitate in a red solution. The mixture was filtered through Celite and the filtrate collected in a Schlenk flask. Volatiles were removed under reduced pressure to afford red–orange solids. The solids were triturated with cold pentane (20 mL) and collected on a fritted glass funnel to yield **5** as a red powder (77 mg, 0.13 mmol, 31%). X-ray quality crystals of **5** were grown via vapor diffusion of hexanes into a concentrated benzene solution. ^{1}H NMR (500 MHz, C_6D_6, 25 °C) δ: 7.35 (br s, 2H, aryl-*H*), 7.23 (t, *J* = 6.5 Hz, 2H, aryl-*H*), 7.07 (t, *J* = 7.3 Hz, 2H, aryl-*H*), 7.00 (t, *J* = 7.3 Hz, 2H, aryl-*H*), 6.28 (br s, 1H, central pyridine-*H*), 6.27 (br s, 1H, central pyridine-*H*), 6.16 (t, *J* = 7.6 Hz, 1H, central pyridine-*H*), 2.91–2.98 (m, 2H, C*H*$(CH_3)_2$), 2.44–2.52 (m, 2H, C*H*$(CH_3)_2$), 1.57 (dd, *J* = 15.4, 7.0 Hz, 6H, CH(C*H*$_3)_2$), 1.28 (dd, *J* = 15.9, 5.5 Hz, 6H, CH(C*H*$_3)_2$), 0.99 (dd, *J* = 12.5, 7.2 Hz, 12H, C*H*$(CH_3)_2$). ^{13}C{^{1}H} NMR (126 MHz, C_6D_6, 25 °C) δ: 131.6 (s, aryl-*C*), 131.5 (s, aryl-*C*), 128.6 (aryl-*C*), 119.6 (s, central pyridine-*C*), 27.3 (d, *J* = 16.2 Hz, C*H*$(CH_3)_2$), 23.3 (d, *J* = 18.2 Hz, C*H*$(CH_3)_2$), 18.9 (d, *J* = 3.2 Hz, CH(C*H*$_3)_2$), 18.8 (s, CH(C*H*$_3)_2$), 18.2 (d, *J* = 3.1 Hz CH(C*H*$_3)_2$), 17.9 (s, CH(C*H*$_3)_2$). ^{31}P{^{1}H} NMR (121 MHz, C_6D_6, 25 °C) δ: 52.71 (v br s), 32.89 (v br s). The HSQC (SI Fig. S19) and HMBC spectra (SI Fig. S20) of **5** indicated that the ^{13}C{^{1}H} NMR resonances of **5** overlapped significantly with that of the NMR solvent used (C_6D_6), which complicated full spectral assignment. Therefore, attempts were made to characterize compound **5** in CD_2Cl_2. However, **5** decomposed in CD_2Cl_2 during the time period of data collection. The spectra collected in CD_2Cl_2 allowed for the following assignments: ^{1}H NMR (500 MHz, CD_2Cl_2, 25 °C) δ: 7.67–7.68 (m, 2H, aryl-*H*), 7.46–7.51 (m, 2H, aryl-*H*), 7.41–7.44 (m, 2H, aryl-*H*), 7.37–7.38 (m, 2H, aryl-*H*), 6.19–6.25 (m, 3H, central pyridine-*H*), 3.04–3.11 (m, 2H, C*H*$(CH_3)_2$), 2.74–2.82 (m, 2H, C*H*$(CH_3)_2$),

1.55–1.60 (m, 6H, CH(CH_3)$_2$), 1.24–1.34 (m, 12H, CH(CH_3)$_2$), 0.96–1.00 (m, 6H, CH(CH_3)$_2$). $^{13}C\{^1H\}$ NMR (126 MHz, CD_2Cl_2, 25 °C) δ: 151.9 (v br s, aryl-*C*), 132.0 (s, aryl-*C*), 131.7 (s, aryl-*C*), 131.3 (br s, aryl-*C*), 128.9 (d, *J* = 4.3 Hz, aryl-*C*), 128.7 (s, aryl-*C*), 119.6 (s, central pyridine-*C*), 118.7 (v br s, central pyridine-*C*), 27.3 (d, *J* = 16.2 Hz, *C*H(CH_3)$_2$), 23.4 (d, *J* = 18.3 Hz, *C*H(CH_3)$_2$), 18.8 (br s, CH(*C*H$_3$)$_2$), 18.2 (s, CH(CH_3)$_2$). IR (ATR, cm^{-1}) ν_{N3}: 2073. Anal. Calcd. for **5**·(0.5 benzene) $C_{32}H_{42}MoP_2N_5$ (%): C, 58.71; H, 6.47; N, 10.70. Found: C, 59.41; H, 6.59; N, 10.37.

2.2.7. Preparation of **6**

A 20 mL scintillation vial was charged with a solution of **5** (22.4 mg, 0.04 mmol) in benzene (10 mL) and a stir bar. With rapid stirring, Me_3SiCl (4.16 μL, 0.03 mmol) was added dropwise from a benzene stock solution (10% by volume, 41.6 μL) using a microsyringe. The reaction mixture was stirred at room temperature for 30 min, during which time it gradually developed into a dark purple-red solution. Volatiles were removed *in vacuo*, providing purple-red solids. The solids were extracted with hexanes and filtered, providing an orange solution. Hexanes were removed under reduced pressure to yield orange solids, which were then recrystallized via benzene/hexanes vapor diffusion to provide red crystals of **6** (6.5 mg, 0.01 mmol, 29%). ^1H NMR (500 MHz, C_6D_6, 25 °C) δ: 7.39 (br s, 2H, aryl-*H*), 7.33 (br s, 2H, aryl-*H*), 7.09 (t, *J* = 6.7 Hz, 2H, aryl-*H*), 7.02 (t, *J* = 6.9 Hz, 2H, aryl-*H*), 6.31 (br s, 2H, central pyridine-*H*), 6.15 (t, *J* = 7.4 Hz, 1H, central pyridine-*H*), 3.46 (br s, 2H, *C*H(CH_3)$_2$), 2.63 (br s, 2H, *C*H(CH_3)$_2$), 1.54–1.56 (m, 6H, CH(*C*H$_3$)$_2$), 1.38–1.40 (m, 6H, CH(*C*H$_3$)$_2$), 1.12–1.16 (m, 6H, CH(*C*H$_3$)$_2$), 1.02 (br s, 6H, CH(*C*H$_3$)$_2$). $^{13}C\{^1H\}$ NMR (126 MHz, C_6D_6, 25 °C) δ: 131.7 (s, aryl-*C*), 131.4 (s, aryl-*C*), 119.1 (s, central pyridine-*C*), 28.0 (d, *J* = 15.7 Hz, *C*H(CH_3)$_2$), 22.7 (d, *J* = 17.7 Hz, *C*H(CH_3)$_2$), 19.6 (s, CH(*C*H$_3$)$_2$), 19.2 (s, CH(*C*H$_3$)$_2$), 18.6 (s, CH(*C*H$_3$)$_2$), 18.2 (s, CH(*C*H$_3$)$_2$). $^{31}P\{^1H\}$ NMR (121 MHz, THF, 25 °C) δ: 60.64 (v br s), 23.05 (v br s). Similar to the case of compound **5**, the HSQC spectrum (SI Fig. S27 and S28) of compound **6** indicated that the $^{13}C\{^1H\}$ NMR resonances of **6** also overlapped significantly with that of the NMR solvent used (C_6D_6), which complicated full spectral assignment. Therefore, attempts were made to characterize compound **6** in CD_2Cl_2. However, compound **6** also demonstrated gradual decomposition in CD_2Cl_2, which prevented prolonged data collection. Data collected in this solvent allowed for the following assignments: ^1H NMR (400 MHz, CD_2Cl_2, 25 °C) δ: 7.67–7.70 (m, 2H, aryl-*H*), 7.47 (t, *J* = 7.3 Hz, 2H, aryl-*H*), 7.36–7.42 (m, 4H, aryl-*H*), 6.28 (br s, 2H, central pyridine-*H*), 6.20 (br s, 1H, central pyridine-*H*), 3.35 (br s, 2H, *C*H(CH_3)$_2$), 2.82 (br s, 2H, *C*H(CH_3)$_2$), 1.51 (dd, *J* = 14.1, 6.7 Hz, 6H, CH(*C*H$_3$)$_2$), 1.31–1.37 (m, 12H, CH(*C*H$_3$)$_2$), 0.94–0.96 (m, 6H, CH(*C*H$_3$)$_2$). $^{13}C\{^1H\}$ NMR (126 MHz, CD_2Cl_2, 25 °C) δ: 151.6 (v br s, aryl-*C*), 131.8 (s, aryl-*C*), 131.7 (s, aryl-*C*), 131.1 (br s, aryl-*C*), 128.7 (s, aryl-*C*), 119.6 (v br s, central pyridine-*C*), 27.7 (br s, *C*H(CH_3)$_2$), 23.0 (br s, *C*H(CH_3)$_2$), 19.3 (d, *J* = 14.2 Hz, CH(*C*H$_3$)$_2$), 18.6 (s, CH(*C*H$_3$)$_2$), 18.6 (s, CH(*C*H$_3$)$_2$). Anal. Calcd. for **6** $C_{29}H_{39}MoP_2N_2Cl$ (%): C, 57.20; H, 6.46; N, 4.60. Found: C, 56.43; H, 6.50; N, 4.56.

2.2.8. Preparation of **7**

A 20 mL scintillation vial was charged with a benzene (5 mL) solution of **5** (20.8 mg, 0.03 mmol) and a stir bar. Stirring was initiated, and a benzene solution (5 mL) of Ph_3SiCl (49.8 mg, 0.17 mmol) was added. After the resulting dark red reaction mixture was stirred at room temperature for 30 min, volatiles were removed under reduced pressure to afford purple solids. The solids were recrystallized by THF/hexanes vapor diffusion, providing X-ray quality dark purple crystals of **7** (10.9 mg, 0.01 mmol, 36%). ^1H NMR (500 MHz, CD_2Cl_2, 25 °C) δ: 7.68 (br s, 3H, aryl-*H*), 7.65 (br s, 2H, aryl-*H*), 7.63 (br s, 3H, aryl-*H*), 7.35–7.52 (m, 15H, NSi(C_6H_5)$_3$), 6.27 (br s, 2H, central pyridine-*H*), 6.19 (br s, 1H, central pyridine-*H*), 3.35 (br s, 2H, *C*H(CH_3)$_2$), 2.81 (br s, 2H, *C*H(CH_3)$_2$), 1.48–1.53 (m, 6H, CH(*C*H$_3$)$_2$), 1.31–1.35 (m, 12H, CH(*C*H$_3$)$_2$), 0.94–0.97 (m, 6H, CH(*C*H$_3$)$_2$). $^{13}C\{^1H\}$ NMR (126 MHz, CD_2Cl_2, 25 °C) δ:135.5 (s, aryl-*C*), 135.3 (s, aryl-*C*), 133.2 (s, NSi(C_6H_5)$_3$), 131.8 (br s, central pyridine-*C*), 131.7 (s, aryl-*C*), 131.2 (NSi(C_6H_5)$_3$), 130.5 (central pyridine-*C*), 128.7 (br s, central pyridine-*C*), 128.6 (s, NSi(C_6H_5)$_3$), 128.3 (s, NSi(C_6H_5)$_3$), 27.7 (*C*H(CH_3)$_2$), 23.0 (*C*H(CH_3)$_2$), 19.4 (CH(*C*H$_3$)$_2$), 19.2 (CH(CH_3)$_2$), 18.6 (CH(CH_3)$_2$). $^{31}P\{^1H\}$ NMR (121 MHz, CD_2Cl_2, 25 °C) δ: 32.39 (v br s), 23.76 (v br s). Anal. Calcd. for **7**·(hexane) $C_{53}H_{68}MoP_2N_2Cl_2Si$ (%): C, 64.30; H, 6.92; N, 2.83. Found: C, 64.30; H, 6.45; N, 3.04.

3. Results and discussion

3.1. Synthesis and metallation of the "P-pyridine-P" ligand platform

Proligand **1** (Scheme 2) can be synthesized in two steps from commercially available starting materials in high yield. Treating a toluene solution of **1** with a single equiv. of Mo(CO)$_3$(MeCN)$_3$ at room temperature cleanly affords a Mo tricarbonyl complex, **2** (Scheme 2). A single signal in the $^{31}P\{^1H\}$ nuclear magnetic resonance (NMR) spectrum at 35.0 ppm (shifted from the free P-pyridine-P ligand **1** at −2.6 ppm) suggests a C_{2v}, C_2 or C_s coordination geometry in solution. The two distinct *C*H(CH_3)$_2$ peaks in the ^1H NMR spectrum rule out a C_{2v} structure. Consistent with the ***σ*-Py** binding mode, the ^1H NMR spectrum of **2** shows central pyridine resonances at 7.74 ppm and 7.21 ppm. The infrared (IR) spectrum of **2** features strong stretches at 1910 cm^{-1}, 1815 cm^{-1} and 1796 cm^{-1}, suggesting retention of all three carbonyl ligands. A single crystal X-ray diffraction (XRD) analysis of **2** corroborates the structural details inferred from solution spectroscopies. The carbonyl ligands coordinate in a facial fashion (Fig. 1) resulting in a *pseudo*-C_s structure, with the P-pyridine-P ligand binding via the nitrogen lone pair.

3.2. Mo complexes supported by the "P-pyridine-P" ligand in the"***σ*-Py**" binding mode

Targeting a CO-free Mo complex, we pursued decarbonylation of **2** through sequential oxidation and photolysis [20(a)]. Tricarbonyl complex **2** can be oxidized with 2 equiv. of silver triflate to yield a Mo^{II} species **3**, accompanied by the spontaneous release of one molecule of CO. Compound **3** exhibits blue-shifted C—O IR stretches at 1966 cm^{-1} and 1898 cm^{-1}, in agreement with reduced backbonding from the oxidized Mo^{II} center. Downfield-shifting of the central pyridine resonances, observed in the ^1H NMR spectrum (7.84–7.82 ppm, 7.79–7.71 ppm and 7.65 ppm), further suggests coordination to a more electron-deficient Mo center. The $^{31}P\{^1H\}$ NMR spectrum of **3** displays two resonances at 112.1 ppm and 52.4 ppm that integrate in a 1:1 ratio, indicating loss of the C_s symmetry. In the $^{13}C\{^1H\}$ NMR spectrum, one of the carbons on the phenylene arm shows an upfield-shifted signal at 123.2 ppm (d, *J* = 36.0 Hz), a phenomenon observed with metal arene interactions in phenylene-linked tris(phosphino)borane ligand platforms [34,40]. The inferred presence of a molybdenum-phenylene interaction in **3**, revealed by the ^{13}C NMR data and apparent asymmetry, was corroborated by single crystal XRD. The Mo center has a close contact to one of the carbons on the phenylene linker in the solid-state structure of **3** (Fig. 1). Accommodating this Mo—C (2.556(2) Å) interaction, the *P*1–Mo–*P*2 angle is bent to 144.12(1)°. For comparison, the *P*1–Mo–*P*2 angle in **2** is 106.08(2)°, which demonstrates the flexibility of the this ligand despite the relatively rigid aryl-aryl linkages.

The reduced Mo—CO π-backbonding in **3** allows further decarbonylation via photolysis [20(a)]. Ultraviolet (UV) irradiation of

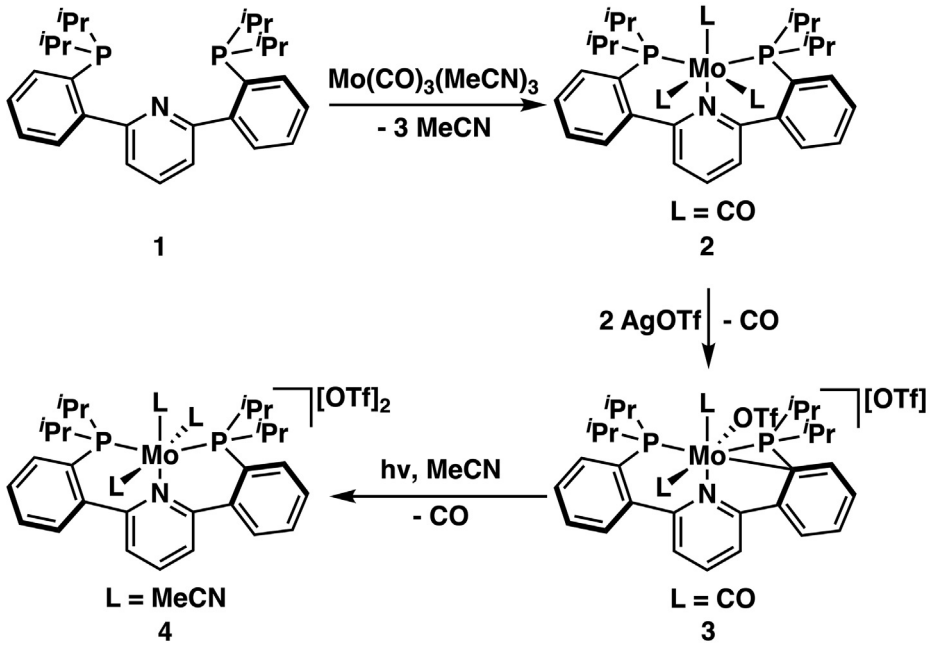

Scheme 2. Synthesis of complexes **2**–**4** in which ligand **1** binds via the pyridine nitrogen σ-framework.

complex **3** leads to a color change from green to brown, then to dark green, accompanied by the disappearance of diamagnetic resonances in the ^{1}H NMR spectrum. The resulting paramagnetic complex **4** showed no C—O stretches in the IR spectrum, indicating complete dissociation of the carbonyl ligands. The solid-state structure of **4** corroborates a meridional Mo^{II} tris(acetonitrile) complex, in which the ***σ*-Py** binding mode is retained (Fig. 1). The loss of the strong-field carbonyl ligands results in decreased d-d splitting, consistent with the observed change of spin state from low-spin in **3** to S = 1 in **4** (Evans method; see Supporting Information). Access to a CO-free Mo^0 complex, a versatile precursor for small molecule activation, was attempted through reduction of **4**, by analogy to the terphenyl-diphosphine system [20(a)]. However, reactions with various chemical reductants have been unsuccessful to date as they gave rise to intractable mixtures comprised primarily of the free P-pyridine-P ligand, **1**.

3.3. Accessing the *π*-Py ligand binding mode

Inspired by the formation of high valent molybdenum nitride species upon the cleavage of N≡N bonds in molybdenum dinitrogen complexes [41], we directly targeted a molybdenum nitrido complex supported by the ligand platform **1** (Scheme 3). Treating dication **4** with two equiv. of tetrabutylammonium (TBA) azide in thawing THF provides nitride azide complex **5** via spontaneous azide thermolysis [29]. Upfield-shifted pyridine proton resonances (6.27 ppm and 6.15 ppm) are observed in the ^{1}H NMR spectrum of **5**, suggesting a new binding mode for the P-pyridine-P ligand. This new coordination is further supported by single crystal XRD, which reveals the pyridine π-system binds Mo in an η^2-fashion. Compared to what is observed in **2**–**4** with nitrogen σ-binding (1.359 Å-1.371 Å), the pyridine N—C distance lengthens to 1.402 (9) Å in **5**, consistent with Mo backdonation into the N—C π^* orbital (Scheme 1, B). In the ^{31}P{^{1}H} NMR spectrum of **5** (SI Fig. S18), two broad resonances at 52.71 ppm and 32.89 ppm are observed. This suggests that a fluxional process, intermediate on the NMR timescale, occurs at room temperature. This fluxionality is attributed to isomerization of the Mo center between the two equivalent η^2-(C, N) binding modes, one of which is represented in the solid state structure (Fig. 2). The installation of a nitride moiety in **5** is confirmed by the solid-state structure, which shows a Mo–N2 distance of 1.6500(1) Å—a value comparable to select Mo^{IV}–nitride bond lengths reported in literature (cf. 1.65 Å) [6(f)].

3.4. Silylation and protonation studies

The formation of high valent transition metal nitride complexes and their subsequent functionalization have been proposed as key steps during catalytic nitrogen fixation [6(c),31,42]. Therefore functionalization of the nitride moiety in **5** was pursued, first by reaction with silyl electrophiles. Treating a benzene solution of **5** with 1 equiv. of trimethylsilyl chloride, affords a nitride chloride complex **6** by salt metathesis. Ligand **1** retains its ***π*-Py** coordination mode in **6**, as evidenced by both the upfield-shifted pyridine ^{1}H NMR resonances (6.31 ppm and 6.16 ppm) and the solid-state structure (Fig. 2). With the addition of an excess (5 equiv.) of triphenylsilyl chloride, silylation of **5** can be achieved to yield imido complex **7**. A single crystal XRD study demonstrates that $SiPh_3$ functionalization occurs at the nitride moiety, lengthening the Mo–N2 distance to 1.772(2) Å, consistent with a Mo–N double bond [43]. The reduced Mo–N bond order in the silyl imido is also reflected by the Mo–N2–Si angle of 162.461(5)° in **7**, which is more significantly bent compared to structurally analogous compounds [43]. In agreement with the disappearance of upfield-shifted pyridine ^{1}H NMR signals, the solid-state structure of **7** shows that ligand **1** has reverted to the ***σ*-Py** binding mode (Fig. 2).

What drives the change of the P-pyridine-P ligand's binding mode between ***σ*-Py** and ***π*-Py**? We speculate that the different requirements for stabilizing Mo centers bearing ligands of different π-basicity may be a contributing factor. In compounds **5** and **6**, the π-acidic metal-pyridine binding mode can form stabilizing donor–acceptor intereactions [28,44] with the azide and chloride ligands. In particular, the strong π-basicity and *trans*-philicity [45–47] of the nitride ligand [7(l)] may have contributed to driving the P-pyridine-P ligand σ to π isomerization. The strongly electron donating nitride results in a more electron rich metal center, which is more prone to donation to π-bound pyridine; the nitrile and CO ligands

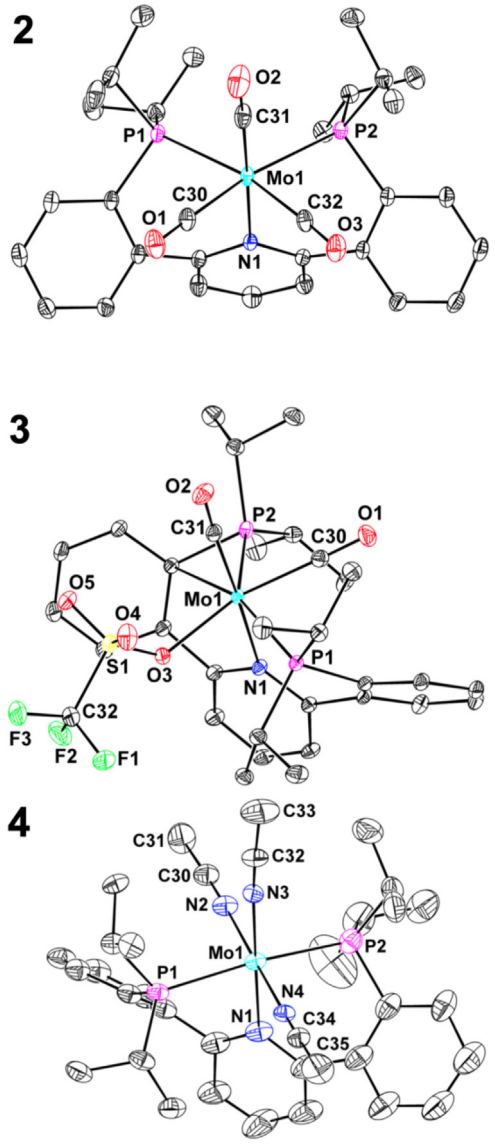

Fig. 1. Solid-state structures of **2**, **3** and **4**. Thermal anisotropic displacement ellipsoids are shown at a 50% probability level. Solvent molecules, counteranions, and hydrogen atoms are omitted for clarity.

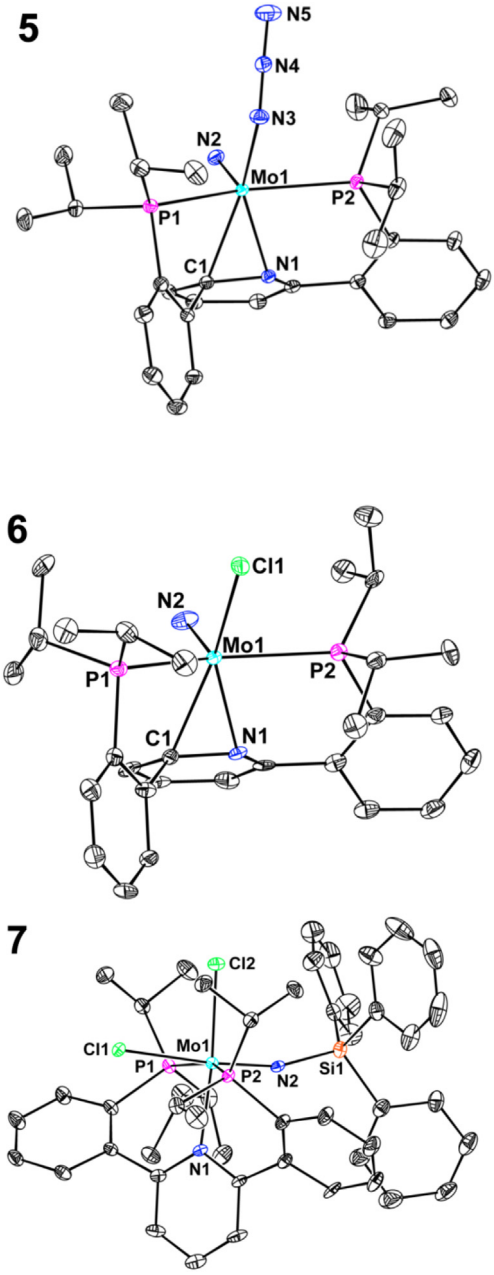

Fig. 2. Solid-state structures of **5**–**7**. Thermal anisotropic displacement ellipsoids are shown at a 50% probability level. Solvent molecules, counteranions, and hydrogen atoms are omitted for clarity.

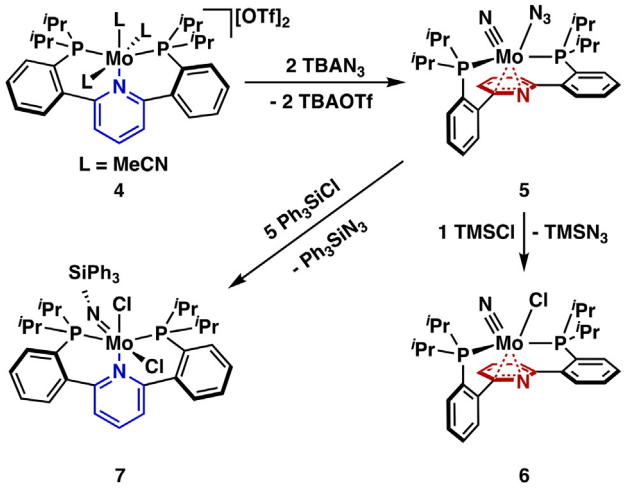

Scheme 3. Synthesis of complexes **5**–**7** in which the ancillary ligand demonstrates variable σ- and π-coordination.

in **2**, **3**, and **4** are not sufficiently donating to favor this pyridine binding mode.

Interested in replacing silyl electrophiles with proton equivalents,[48] we investigated the reaction of **6** with Brookhart's acid ($HBAr^F_4$). Upon the addition of 1 equiv. of $HBAr^F_4$ (as an ether solution) to a thawing benzene solution of **6**, the generation of a mixture of paramagnetic and diamagnetic species was detected by ^{1}H NMR spectroscopy. Preliminary crystallographic characterization allowed two of the products in this mixture to be identified as a Mo^V nitride chloride monocation (**8**) and a Mo^{III} acetonitrile dichloride monocation (**9**) (Scheme 4, SI Figs. S42 and S43). The detection of these species can be rationalized via disproportionation [49] following the addition of protons: **6** may potentially serve as a one electron reductant, thereby affording the Mo^{III} and Mo^V species (Scheme 4). In the ^{1}H NMR spectrum of the protonation reaction mixture (SI Fig. S41),

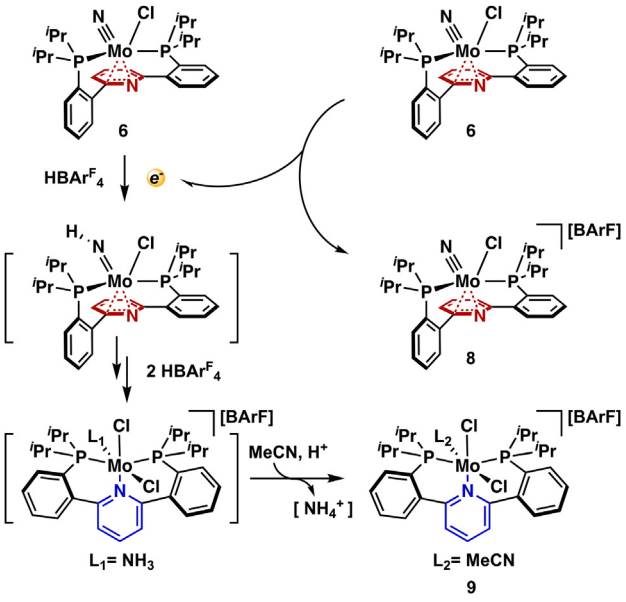

Scheme 4. Postulated disproportionation pathway during protonation with $HBAr^F_4$.

a 1:1:1 triplet resonance (5.78 ppm) with a coupling constant of J = 53.1 Hz was observed—spectroscopic features characteristic of protons split by ^{14}N (S = 1). Relative integration of this triplet with respect to other diamagnetic ^1H NMR signals precludes its assignment as protonated ligand (**1-H$^+$**, the pyridinium salt of **1**) or a Mo species supported by **1-H$^+$**. Taken together, these preliminary data seem most consistent with the release of ammonia (and subsequent protonation to ammonium) to balance the loss of the nitride ligand required upon formation of **9** (Scheme 4). This disproportionation reactivity *en route* to ammonia generation is notable given its analogy to intermetallic electron transfer proposed in catalytic N_2 fixation by closely related Mo-pincer complexes [50].

4. Conclusions

In summary, complexes **2**–**9** demonstrate that the flexible diphenyl pyridine pincer ligand **1** is capable of supporting Mo centers across five formal oxidation states, and various coordination numbers and spin states. Accommodating the electronic and geometric requirements engendered by these Mo centers, the ligand **1** can adaptively switch its coordination mode between pyridine nitrogen σ-donation and binding through the pyridine π-system. Preliminary investigation into protonation reactions suggests that electrons can shuffle between the protonated and un-protonated Mo^{IV} species. This proposed disproportionation mechanism is supported by the generation of Mo^{III} and Mo^{V} complexes, as well as the spectroscopic detection of NH_4^+ after protonation with $HBAr^F_4$. This reactivity manifold demonstrates an inter-molybdenum electron transfer mechanism during the protonolysis of a terminal nitride, and suggests that such a process may be a general phenomenon in nitrogen reduction catalyzed by molybdenum-PNP complexes [6(c),46].

Declaration of interests

The authors declare that they have no known competing financial interests or personal relationships that could have appeared to influence the work reported in this paper.

Acknowledgements

We thank Michael K. Takase and Lawrence M. Henling for crystallographic assistance, David Vandervelde for help with NMR experiments and Harry Gray for stimulating discussions. R.W. is grateful for a Caltech Summer Undergraduate Research Fellowship (SURF), and J.A.B. for an NSF pre-doctoral fellowship. We thank Caltech and the NSF (CHE-1800501) for funding. The Bruker KAPPA APEXII X-ray diffractometer was purchased via an NSF CRIF:MU award to Caltech, CHE-063-9094. The 500 MHz NMR spectrometer was purchased via an NIH award, RR027690.

Appendix A. Supplementary data

CCDC entries 1846385, 1846659, 1846660, 1846813, 1846889, 1846828 and 1998474 contain the supplementary crystallographic data for **2**, **3**, **4**, **5**, **6**, **7** and **8**, respectively. These data can be obtained free of charge via http://www.ccdc.cam.ac.uk/conts/retrieving.html, or from the Cambridge Crystallographic Data Centre, 12 Union Road, Cambridge CB2 1EZ, UK; fax: (+44) 1223-336-033; or e-mail:deposit@ccdc.cam.ac.uk. Supplementary data to this article can be found online at https://doi.org/10.1016/j.poly.2020.114631.

References

[1] (a) G. van Koten, R.J.M.K. Gebbink, Dalton Trans. 40 (2011) 8731–8732;
(b) G. van Koten, D. Milstein, Organometallic pincer hemistry, Topics in Organometallic Chemistry series, Springer, Heidelberg, 2013;
(c) G. van Koten, R.A. Gossage, The Privileged Pincer-Metal Platform: Coordination Chemistry & Applications, Topics in Organometallic Chemistry series, Springer, Berlin, 2016;
(d) S.P. Semproni, C. Milsman, P.J. Chirik, J. Am. Chem. Soc. 136 (2014) 9211–9224;
(e) I. Arenas, O. Boutureira, M.I. Matheu, Y. Díaz, S. Castillón, Eur. J. Org. Chem. 17 (2015) 3666–3669.
[2] (a) M.H. Rietveld, D.M. Grove, G. van Koten, New J. Chem. 21 (1997) 751–771;
(b) D. Morales-Morales, C.M. Jensen (Eds.), The Chemistry of Pincer Compounds, Elsevier, Amsterdam, 2007;
(c) G. van Koten, M. Albrecht, Angew. Chem. Int. Ed. 49 (2001) 3750–3781;
(d) M.E. van der Boom, D. Milstein, Chem. Rev. 103 (2003) 1759–1792;
(e) D. Benito-Garagorri, K. Kirchner, Acc. Chem. Res. 41 (2008) 201–213;
(f) J. Choi, A.H.R. MacArthur, M. Brookhart, A. Goldman, A.S. Chem, Rev. 111 (2011) 1761–1779;
(g) N. Selander, K.J. Szabó, Chem. Rev. 111 (2011) 2048–2076;
(h) P.J. Chirik, K. Wieghardt, Science. 327 (2012) 794–795;
(i) B. Bichler, C. Holzhacker, B. Stöger, M. Puchberger, L.F. Veiros, K. Kirchner, Organometallics. 32 (2013) 4114–4121.
[3] C.J. Moulton, B.L. Shaw, J. Chem. Soc., Dalton Trans. 11 (1976) 1020–1024.
[4] (a) G. van Koten, K. Timmer, J.G. Noltes, A.L. Spek, J. Chem. Soc., Chem. Commun. 6 (1978) 250–252;
(b) G. van Koten, J.T.B.H. Jastrzebski, J.G. Noltes, A.L. Spek, J.C. Schoone, J. Organomet. Chem. 148 (1978) 233–245.
[5] (a) M. Ohff, A. Ohff, M. van der Boom, D. Milstein, J. Am. Chem. Soc. 119 (1997) 11687–11688;
(b) D. Morales-Morales, C. Grause, K. Kasaoka, R. Redón, R.E. Cramer, C.M. Jensen, Inorg. Chim. Acta. 300 (2000) 958–963;
(c) R.B. Bedford, S.M. Draper, P.N. Scully, S.L. Welch, New J. Chem. 24 (2000) 745–747;
(d) I.G. Jung, S.U. Son, K.H. Park, K.C. Chung, J.W. Lee, Y.K. Chung, Organometallics. 22 (2003) 4715–4720;
(e) K. Takenaka, M. Minakawa, Y. Uozumi, J. Am. Chem. Soc. 127 (2005) 12273–12281;
(f) B. Soro, S. Stoccoro, G. Minghetti, A. Zucca, M.A. Cinellu, M. Manassero, S. Gladiali, Inorg. Chim. Acta. 359 (2006) 1879–1888.
[6] (a) K. Arashiba, Y. Miyake, Y. Nishibayashi, Nat. Chem. 3 (2011) 120–125;
(b) E. Kinoshita, K. Arashiba, S. Kuriyama, Y. Miyake, R. Shimazaki, H. Nakanishi, Y. Nishibayashi, Organometallics. 31 (2012) 8437–8443;
(c) H. Tanaka, K. Arashiba, S. Kuriyama, A. Sasada, K. Nakajima, K. Yoshizawa, Y. Nishibayashi, Nat. Commun. 5 (2014) 3737;
(d) S. Kuriyama, K. Arashiba, K. Nakajima, H. Tanaka, N. Kamaru, K. Yoshizawa, Y. Nishibayashi, J. Am. Chem. Soc. 136 (2014) 9719–9731;
(e) S. Kuriyama, K. Arashiba, K. Nakajima, H. Tanaka, K. Yoshizawa, Y. Nishibayashi, Chem. Sci. 6 (2015) 3940–3951;
(f) K. Arashiba, E. Kinoshita, S. Kuriyama, A. Eizawa, K. Nakajima, H. Tanaka, K. Yoshizawa, Y. Nishibayashi, J. Am. Chem. Soc. 137 (2015) 5666–5669;

(g) A. Eizawa, K. Arashiba, H. Tanaka, S. Kuriyama, Y. Matsuo, K. Nakajima, K. Yoshizawa, Y. Nishibayashi, Nat. Commun. 8 (2017) 14874.
[7] (a) M.G. Scheibel, Y. Wu, A.C. Stückl, L. Krause, E. Carl, D. Stalke, B. de Bruin, S. Schneider, J. Am. Chem. Soc. 135 (2013) 17719–17722;
(b) I. Klopsch, M. Finger, C. Würtele, B. Milde, D.B. Werz, S. Schneider, J. Am. Chem. Soc. 136 (2014) 6881–6883;
(c) M.G. Scheibel, J. Abbenseth, M. Kinauer, F.W. Heinemann, C. Würtele, B. de Bruin, S. Schneider, Inorg. Chem. 54 (2015) 9290–9302;
(d) J. Abbenseth, M. Finger, C. Würtele, M. Kasanmascheff, S. Schneider, Inorg. Chem, Front. 3 (2016) 469–477;
(e) B.M. Lindley, R.S. van Alten, M. Finger, F. Schendzielorz, C. Würtele, A.J.M. Miller, I. Siewert, S. Schneider, J. Am. Chem. Soc. 140 (2018) 7922–7935;
(f) Q.J. Bruch, B.M. Lindley, B. Askevold, S. Schneider, A.J.M. Miller, Inorg. Chem. 57 (2018) 1964–1975;
(g) I. Klopsch, F. Schendzielorz, C. Volkmann, C. Würtele, S. Schneider, Z. Anorg, Allg. Chem. 644 (2018) 916–919;
(h) F. Schendzielorz, M. Finger, J. Abbenseth, C. Würtele, V. Krewald, S. Schneider, Angew. Chem. Int. Ed. 58 (2019) 830–834;
(i) G.A. Silantyev, M. Förster, B. Schluschaß, J. Abbenseth, C. Wgrtele, C. Volkmann, M.C. Holthausen, S. Schneider, Angew. Chem. Int. Ed. 56 (2017) 5872–5876;
(j) B. Schluschaß, J. Abbenseth, S. Demeshko, M. Finger, A. Franke, C. Herwig, C. Würtele, I. Ivanovic-Burmazovic, C. Limberg, J. Telser, S. Schneider, Chem. Sci. 10 (2019) 10275–10282;
(k) Q.J. Bruch, G.P. Connor, C.-H. Chen, P.L. Holland, J.M. Mayer, F. Hasanayn, A. J.M. Miller, J. Am. Chem. Soc. 141 (2019) 20198–20208;
(l) B.M. Lindley, Q.J. Bruch, P.S. White, F. Hasanayn, A.J.M. Miller, J. Am. Chem. Soc. 139 (2017) 5305–5308.
[8] G. van Koten, Pure & Appl. Chem. 61 (1989) 1681–1694.
[9] (a) H. Grützmacher, Angew. Chem., Int. Ed. 47 (2008) 1814–1818;
(b) C. Gunanathan, D. Milstein, Acc. Chem. Res. 44 (2011) 588–602;
(c) M. Vogt, M. Gargir, M.A. Iron, Y. Diskin-Posner, Y. Ben-David, D. Milstein, Chem. Eur. J. 18 (2012) 9194–9197.
[10] (a) J.C. Jeffrey, T.B. Rauchfuss, Inorg. Chem. 18 (1979) 2658–2666;
(b) R. Lindner, B. van den Bosch, M. Lutz, J.N.H. Reek, J.I. van der Vlugt, Organometallics. 30 (2011) 499–510.
[11] (a) D.P. Barondeau, C.J. Kassmann, C.K. Bruns, J.A. Tainer, E.D. Getzoff, Biochemistry. 43 (2004) 8038–8047;
(b) J. Wuerges, J.W. Lee, Y.I. Yim, H.S. Yim, S.O. Kang, K.D. Carugo, Proc. Natl. Acad. Sci. U. S. A. 101 (2004) 8569–8574.
[12] (a) E.B. Springman, E.L. Angleton, H. Birkedal-Hansen, H.E. van Wart, Proc. Natl. Acad. Sci. U. S. A. 87 (1990) 364–368;
(b) H.E. van Wart, H. Birkedal-Hansen, Proc. Natl. Acad. Sci. U. S. A. 87 (1990) 5578–5582.
[13] T.G. Traylor, C.K. Chang, J. Geibel, A. Berzinis, T. Mincey, J. Cannon, J. Am. Chem. Soc. 101 (1979) 6716–6731.
[14] T.J.M. de Bruin, L. Magna, P. Raybaud, H. Toulhoat, Organometallics. 22 (2003) 3404–3413.
[15] (a) J.I. van der Vlugt, J.M. Bonet, A.M. Mills, A.L. Spek, D. Vogt, Tetrahedron Lett. 44 (2003) 4389–4392;
(b) J.I. van der Vlugt, R. Sablong, P.C.M.M. Magusin, A.M. Mills, A.L. Spek, D. Vogt, Organometallics. 23 (2004) 3177–3183;
(c) M.M.P. Grutters, J.I. van der Vlugt, Y. Pei, A.M. Mills, M. Lutz, A.L. Spek, C. Müller, C. Moberg, D. Vogt, Adv. Synth. Catal. 351 (2009) 2199–2208.
[16] (a) A. Bader, E. Lindner, Coord. Chem. Rev. 108 (1991) 27–110;
(b) C.S. Slone, D.A. Weinberger, C.A. Mirkin, Prog. Inorg. Chem. 48 (1999) 233–350;
(c) P. Braunstein, F. Naud, Angew. Chem. Int. Ed. 40 (2001) 680–699;
(d) G.L. Moxham, H.E. Randell-Sly, S.K. Brayshaw, R.L. Woodward, A.S. Weller, M.C. Willis, Angew. Chem. Int. Ed. 45 (2006) 7618–7622.
[17] (a) J. Zhang, G. Leitus, Y. Ben-David, D. Milstein, J. Am. Chem. Soc. 127 (2005) 10840–10841;
(b) C. Gunanathan, Y. Ben-David, D. Milstein, Science. 317 (2007) 790–792.
[18] A. Velian, S. Lin, A.J.M. Miller, M.W. Day, T. Agapie, J. Am. Chem. Soc. 132 (2010) 6296–6297.
[19] (a) S. Lin, M.W. Day, T. Agapie, J. Am. Chem. Soc. 133 (2011) 3828–3831;
(b) D.E. Herbert, N.C. Lara, T. Agapie, Chem. Eur. J. 19 (2013) 16453–16460;
(c) K.T. Horak, A. Velian, M.W. Day, T. Agapie, Chem. Commun. 50 (2014) 4427–4429;
(d) K.T. Horak, D.G. VanderVelde, T. Agapie, Organometallics. 34 (2015) 4753–4765;
(e) G.A. Edouard, P. Kelley, D.E. Herbert, T. Agapie, Organometallics. 34 (2015) 5254–5277.
[20] (a) J.A. Buss, G.A. Edouard, C. Cheng, J. Shi, T. Agapie, J. Am. Chem. Soc. 136 (2014) 11272–11275;
(b) J.A. Buss, T. Agapie, Nature. 529 (2016) 72–75.
[21] K.T. Horak, D.G. VanderVelde, T. Agapie, Organometallics. 34 (2015) 4753–4765.
[22] (a) J.T. Henthorn, T. Agapie, Inorg. Chem. 55 (2016) 5337–5342;
(b) K.T. Horak, T. Agapie, J. Am. Chem. Soc. 138 (2016) 3443–3452.
[23] J.A. Buss, D.G. VanderVelde, T. Agapie, J. Am. Chem. Soc. 140 (2018) 10121–10125.
[24] J.A. Buss, T. Agapie, J. Am. Chem. Soc. 138 (2019) 16466–16477.
[25] J.A. Buss, G.A. Bailey, J. Oppenheim, D.G. VanderVelde, W.A. Goddard, T. Agapie, J. Am. Chem. Soc. 141 (2019) 15664–15674.
[26] C.H. Low, J.N. Rosenberg, M.A. Lopez, T. Agapie, J. Am. Chem. Soc. 140 (2018) (1910) 11906–11911.
[27] J.T. Henthorn, S. Lin, T. Agapie, J. Am. Chem. Soc. 137 (2015) 1458–1464.
[28] J.A. Buss, P.H. Oyala, T. Agapie, Angew. Chem. Int. Ed. 56 (2017) 14502–14506.
[29] J.A. Buss, C. Cheng, T. Agapie, Angew. Chem. Int. Ed. 57 (2018) 9670–9674.
[30] (a) S. Schneider, J. Meiners, B. Askevold, Eur. J. Inorg. Chem. 3 (2012) 412–429;
(b) V.T. Annibale, D. Song, RSC Adv. 3 (2013) 11432–11449.
[31] Y. Nishibayashi, Inorg. Chem. 54 (2015) 9234–9237.
[32] (a) J. Chatt, A.J. Pearman, R.L. Richards, Nature. 253 (1975) 39–40;
(b) J. Chatt, A.J. Pearman, R.L. Richards, J. Chem. Soc., Dalton Trans. 6 (1977) 1852–1860.
[33] (a) D.V. Yandulov, R.R. Schrock, Science. 301 (2003) 76–78;
(b) V. Ritleng, D.V. Yandulov, W.W. Weare, R.R. Schrock, A.S. Hock, W.M. Davis, J. Am. Chem. Soc. 126 (2004) 6150–6163;
(c) R.R. Schrock, Acc. Chem. Res. 38 (2005) 955–962;
(d) W.W. Weare, X. Dai, M.J. Byrnes, J.M. Chin, R.R. Schrock, P. Müller, Proc. Nati. Acad. Sci. U.S.A. 103 (2006) 17099–17106;
(e) R.R. Schrock, Angew. Chem., Int. Ed. 47 (2008) 5512–5522.
[34] M.-E. Moret, J.P. Peters, Angew. Chem. Int. Ed. 50 (2011) 2063–2067.
[35] A.B. Pangborn, M.A. Giardello, R.H. Grubbs, R.K. Rosen, F.J. Timmers, Organometallics. 15 (1996) 1518–1520.
[36] D.P. Tate, W.R. Knipple, J.M. Angl, Inorg. Chem. 1 (1962) 433–434.
[37] M. Brookhart, B. Grant, A.F. Volpe, Organometallics. 11 (1992) 3920–3922.
[38] G.R. Fulmer, A.J.M. Miller, N.H. Sherden, H.E. Gottlieb, A. Nudelman, B.M. Stoltz, J.E. Bercaw, K.I. Goldberg, Organometallics. 29 (2010) 2176–2179.
[39] X. Feng, W. Pisula, K. Mullen, J. Am. Chem. Soc. 129 (2007) 14116–14117.
[40] M.J. Chalkley, J.C. Peters, Angew. Chem. Int. Ed. 55 (2016) (1998) 11995–12001.
[41] (a) C.E. Laplaza, C.C. Cummins, Science. 268 (1995) 861–863;
(b) A. Katayama, T. Ohta, Y. Wasada-Tsutsui, T. Inomata, T. Ozawa, T. Ogura, H. Masuda, Angew. Chem. Int. Ed. 58 (2019) 11279–11284;
(c) K. Arashiba, A. Eizawa, H. Tanaka, K. Nakajima, K. Yoshizawa, Y. Nishibayashi, Bull. Chem. Soc. Jpn. 90 (2017) 1111–1118.
[42] (a) B. Askevold, J.T. Nieto, S. Tussupbayev, M. Diefenbach, E. Herdtweck, M.C. Holthausen, S. Schneider, Nat. Chem. 3 (2011) 532–537;
(b) M.M. Rodriguez, E. Bill, W.W. Brennessel, P.L. Holland, Science. 334 (2011) 780–783;
(c) Y. Nishibayashi, Nat. Chem. 3 (2011) 502–504.
[43] (a) N.C. Mösch-Zanetti, R.R. Schrock, W.M. Davis, K. Wanninger, S.W. Seidel, M.B. O'Donoghue, J. Am. Chem. Soc. 119 (1997) 11037–11048;
(b) B.L. Yonke, J.P. Reeds, P.P. Fontaine, P.Y. Zavalij, L.R. Sita, Organometallics. 33 (2014) 3239–3242;
(c) Q. Liao, N. Saffon-Merceron, N. Mézailles, Angew. Chem. Int. Ed. 53 (2014) 14206–14210;
(d) Q. Liao, A. Cavaillé, N. Saffon-Merceron, N. Mézailles, Angew. Chem. Int. Ed. 55 (2016) 11212–11216;
(e) L.M. Duman, W.S. Farrell, P.Y. Zavalij, L.R. Sita, J. Am. Chem. Soc. 138 (2016) 14856–14859.
[44] K.G. Caulton, New J. Chem. 18 (1994) 25–41. (b) K.T. Horak, T. Agapie, J. Am. Chem. Soc. 138 (2016) 3443–3452.
[45] A.C. Tsipis, Dalton Trans. 48 (2019) 1814–1822.
[46] B.M. Lindley, Q.J. Bruch, P.S. White, F. Hasanayn, A.J.M. Miller, J. Am. Chem. Soc. 129 (2017) 5305–5308.
[47] P.D. Lyne, D.M.P. Mingos, J. Chem. Soc., Dalton Trans. 10 (1995) 1635–1643.
[48] (a) J. Chakraborty, U. Mandal, I. Ghiviriga, K.A. Abboud, A.S. Veige, Chem. Eur. J. 25 (2019) 14059–14063;
(b) Y. Ashida, K. Arashiba, K. Nakajima, Y. Nishibayashi, Nature 568 (2019) 536–540.
[49] H. Kunkely, A. Volgler, Angew. Chem. Int. Ed. 49 (2010) 1591–1593.
[50] H. Tanaka, Y. Nishibayashi, K. Yoshizawa, Acc. Chem. Res. 49 (2016) 987–995.